



The Fundamentals And The Capabilities Of Si-Bipolar Junction Transistors

Abdelfatteh Cherif

Assistant Professor

Physics Department, Al Jamoum University College, Kingdom of SAUDI ARABIA

Institut Préparatoire aux Etudes d'Ingénieurs de Kairouan, TUNISIA

Laboratoire de physique quantique et statistique, Université de Monastir, TUNISIA

Abstract: Consider the energy-band diagram of the n-p-n bipolar transistor in the forward active mode, at which the emitter-base junction is forward biased and the collector-base junction is reverse biased. The forward-biased junction voltage reduces the potential barrier at the emitter-base junction and triggers the injection of electrons from the emitter to the base. The reduced potential barrier also helps holes diffuse through the forward-biased emitter-base junction into the emitter region. The supply of electrons at the emitter contact provides the emitter current, and the supply of holes at the base contact results in the base current. Since the collector junction is reverse biased, the energy band bends down and prevents hole injection from the base to the collector. The electrons injected into the base, however, are assisted by the field in the collector-base depletion region and are swept to the collector. The collection of electrons at the collector contact gives rise to the collector current has been undertaken to investigate

Index Terms – bipolar junction transistor (BJT), forward-active mode, inverse-active mode, transistor collector.

I. INTRODUCTION

The bipolar junction transistor (BJT) was invented by a research team at Bell Laboratories in 1947. In 1948 John Bardeen and Walter Brattain announced the development of the point-contact transistor (Bardeen and Brattain, 1948). In the following year William Shockley's paper on junction diodes and transistors was published (Shockley, 1949). The development of conventional bipolar theory and fabrication was very active from the 1950s to 1960s. Because of the need for low power dissipation and high packaging density for VLSI applications, major R&D efforts focused on the study of complementary metal-oxide semiconductor (CMOS) field-effect transistors in the 1970s. R&D in BIT technology became dormant for approximately a decade. The activity of bipolar development was revitalized when the polysilicon emitter was introduced in the BIT at mM's Watson lab in the early 1980s. Conventional bipolar theory was reexamined and improved for advanced polysilicon bipolar transistor design and fabrication.

II. DC CHARACTERISTICS AND SIMULATION

The current-voltage characteristics during forward-active, inverse-active modes of operation and for room temperature are presented in this section. Physical mechanisms of emitter current crowding, base pushout, collector current spreading, will be illustrated in detail. Device simulation results are given in conjunction with qualitative analysis. Device simulations are conducted to provide physical insight into device operation, not to duplicate experimental data. The use of device simulation is also useful for model development, process diagnosis, and device design in a Technology CAD environment.

II.1 Current-Voltage Characteristics/or Forward-Active and Saturation Operation

When the bipolar transistor is in the forward-active mode, electrons diffuse through the forward-biased emitter-base junction into the base, and holes diffuse through the forward-biased junction into the emitter. The injected electrons in the base are swept by the field at the collector-base junction to the collector. When the bipolar transistor is in the saturation mode, electrons are injected from both the emitter and collector regions and holes are injected from the base contact to supply recombination currents in the emitter, base, and collector. In this mode of operation, the collector current is decreased and the base current is increased, resulting in a significant reduction of current gain in saturation. This result is consistent with physical insight into minority carrier concentration distribution in the base. The use of a 2-D device simulator provides physical insight into device operation in any mode. The internal physical responses such as electron and hole concentrations, current vectors, and potential contours of the BJT can be obtained from device simulation. Physical simulation is useful for analyzing the impact of different modes of operation on a device's dc, and transient behaviors as well as for designing high-performance transistors. We will now simulate a bipolar transistor. A generic advanced BJT cross section was constructed by incorporating common features of many state-of-the-art transistors reported in the literature by Konaka et al [1] and Tang et al [2]. Only a half cross section and doping profile is needed due to the cross-section's symmetry. The cross section of the BJT and its vertical doping profile are shown in Figs. 1 and 2, respectively. The BJT has a 1- μm emitter width ($W_E/2 = 0.5\mu\text{m}$), a 0.15- μm emitter junction depth, a 0.3- μm base junction depth, and a 0.7- μm epilayer depth. The doping profiles are assumed Gaussian for the emitter, Gaussian for the base, and uniform for the epilayer collector. The peak dopings are 2×10^{20}

cm^{-3} , $9 \times 10^{17} \text{ cm}^{-3}$, and $2 \times 10^{16} \text{ cm}^{-3}$ in the emitter, intrinsic base, and epilayer, respectively. The lateral emitter-base spacing was designed to avoid sidewall tunneling and perimeter punch-through in the BJT [3].

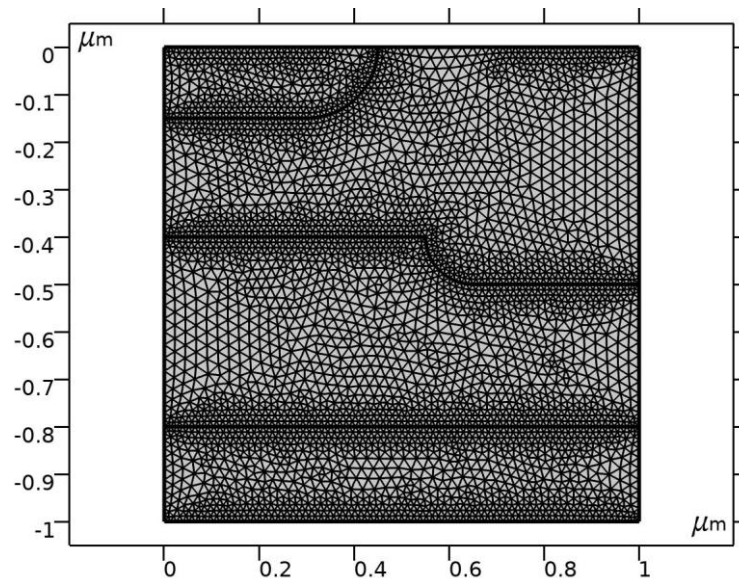


FIGURE 1. Cross section of BJT used in device simulation.

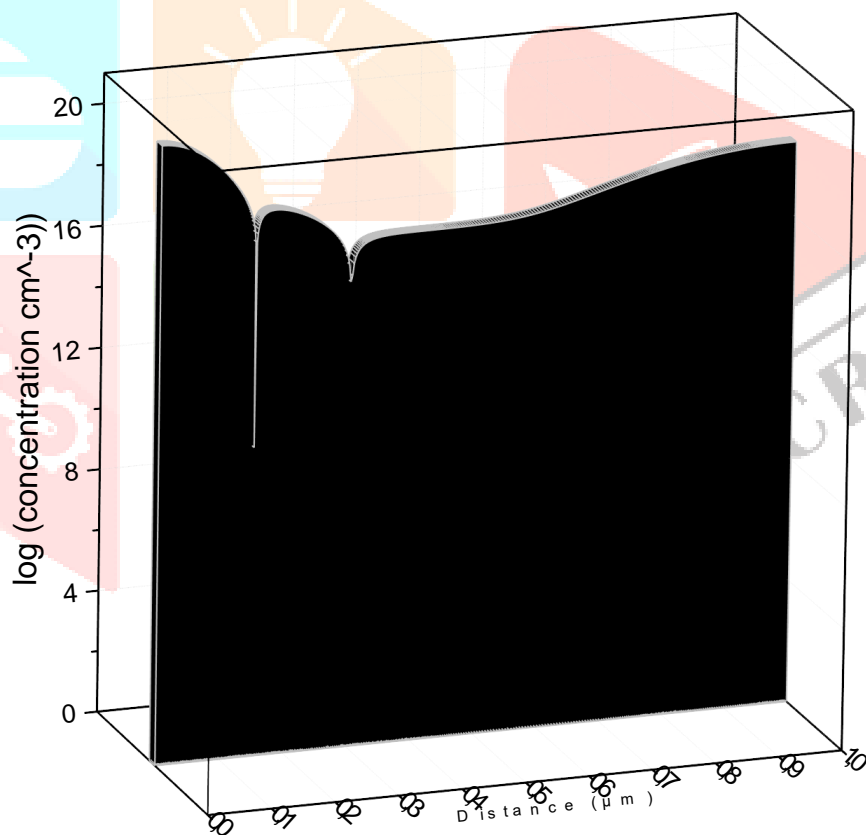


FIGURE 2. Vertical doping profile of the BJT.

The emitter dopant lateral straggles are assumed to be 75% of the vertical straggles for the emitter-sidewall lateral diffusion [4]. The physical models used in device simulation include Shockley-Read-Hall recombination, Auger recombination, concentration- and field-dependent mobilities, concentration-dependent lifetimes, and band-gap narrowing. The device parameters used include $\tau_{n0} = 1 \times 10^{-7} \text{ s}$, $\tau_{p0} = 1 \times 10^{-7} \text{ s}$, $N_c = 2.8 \times 10^{18} \text{ cm}^{-3}$, $N_v = 1.04 \times 10^{18} \text{ cm}^{-3}$, $N_{SRHN} = 5 \times 10^{16} \text{ cm}^{-3}$, $N_{SRHH} = 5 \times 10^{16} \text{ cm}^{-3}$, $C_n = 2.8 \times 10^{-31}$, $C_p = 9.9 \times 10^{-32}$, $\epsilon_{Si} = 11.8$, and $E_G = 1.08 \text{ eV}$. Figure 3 shows a typical Gummel plot of an n-p-n bipolar transistor using the COMSOL Multiphysics simulation. In Fig. 3.6 the collector and base currents increase with base-emitter voltage. At low base-emitter voltages, the base current is relatively high due to contribution of space-charge recombination. At high base-emitter voltages, significant ohmic resistance effects ($I_B R_B + I_C R_C$) are observed.

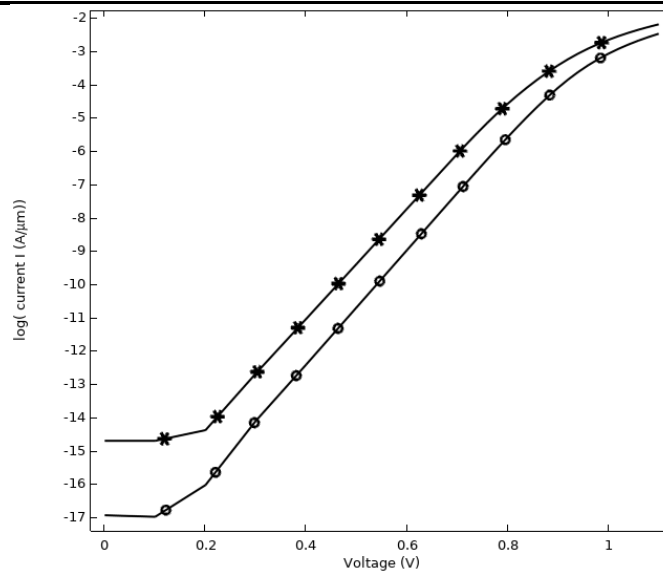


FIGURE 3. Collector (*) and base (o) currents versus base-emitter bias simulated.

Figure 4 shows hole current vectors in saturation (base-collector $V_{BC}=0.6$ V). In this mode of operation, holes are injected into the emitter and collector. The base current is increased and the current gain is decreased.

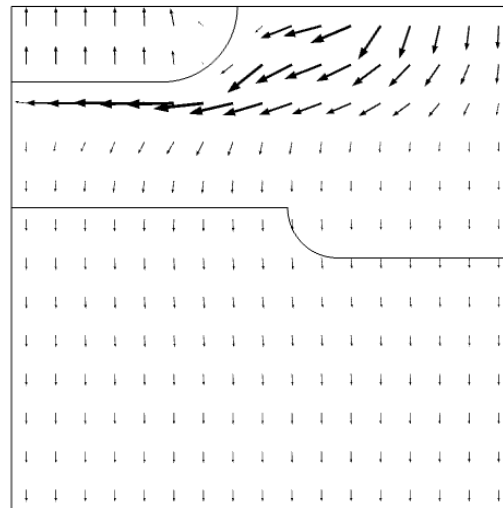


FIGURE 4. Current vectors of the BJT in saturation.

II.2 Current-Voltage Characteristics for Revers-Active Operation

If we now interchange the collector and emitter terminals, then the two junctions effectively interchange roles. When the collector-base junction is forward biased and the emitter-base junction is reverse biased, this is known as reverse-active operation of the BJT. Furthermore, when both collector-base and emitter-base junctions are forward biased and the forward-biased collector-base junction has a greater value than that of the emitter-base junction, this condition is reverse saturation. For modern bipolar transistors, the emitter and collector doping profiles are not balanced or interchangeable. The emitter, which has a Gaussian profile, is heavily doped to increase the emitter injection efficiency and reduce the emitter resistance spreading is indicated by the horizontal component of current density vectors underneath the extrinsic base.

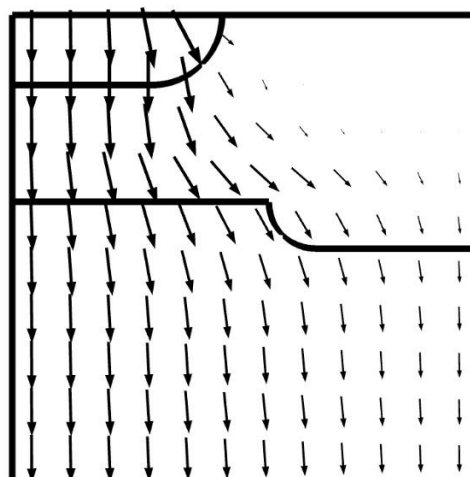


FIGURE 5. Plot of electron current vectors. The collector contact is at the bottom of the buried collector.

Note that Fig. 5 qualitatively shows where the multidimensional collector currents occur, but it does not lend itself to a quantitative estimation of the magnitude of these currents. The grid in Fig. 5 is uniform (for better simulation accuracy) and is dense at emitter, base and emitter-base junctions because of the position-dependent doping density at these regions. The magnitudes of the current density vectors at the grid points which are sparsely located are enhanced when compared to those of dense grid points. The effect of electric field on the current distribution in the epitaxial collector can be seen by putting the collector contact on the right side of the BJT. Figure 6 shows a BJT simulation of the current density vectors for a right-side-collector contact, with $V_{CE} = 2.0$ V and $V_{BE} = 0.9$ V, the same bias as that of Fig. 5. Although there are great differences in the current vectors in the buried collector (due to lateral ohmic drop), all the current in the intrinsic BJT remains virtually the same. The magnitudes of the vertical and lateral current density vectors in Fig. 5 and Fig. 6 are typically within 0.5% of each other. This indicates that the electric field from the right-side collector contact only controls the current flow in the buried-collector region, and that it does not significantly affect the lateral flow. Thus, there is no significant drift component in the collector spreading mechanism.

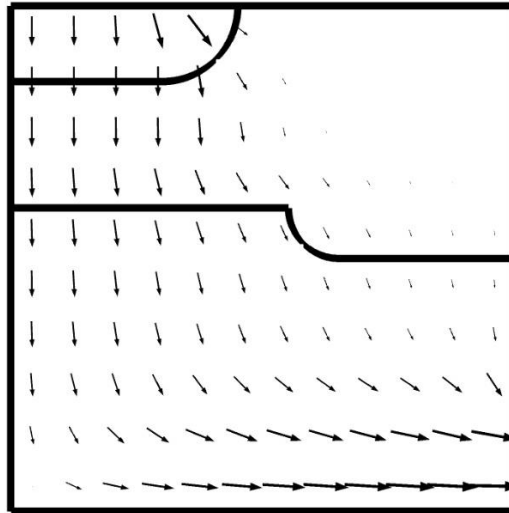


FIGURE 6. Plot of electron current vectors. The collector contact is at the bottom of the buried collector.

A 1-D collector transistor was simulated in order to isolate the effects of collector spreading in the advanced BJT operation [7,8]. This 2-D collector BJT, shown in Fig. 7, has the same emitter and base regions as the 2-D BJT in Fig. 5. However, below the extrinsic base region of the 1-D collector transistor, the epitaxial and buried-collector regions are replaced with SiO_2 . This forces the collector current to flow solely in the vertical direction below the intrinsic base, hence the name 1-D collector transistor.

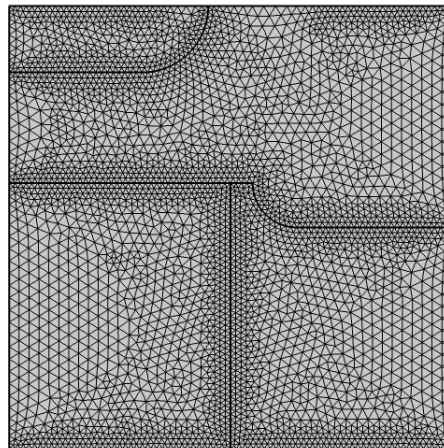


FIGURE 7. Design of 1-D collector BJT cross section to isolate the 2-D collector spreading.

III. CONCLUSION

A collector transistor was simulated in order to isolate the effects of collector spreading in the advanced BJT operation. This collector BJT. However, below the extrinsic base region of the collector transistor, the epitaxial and buried-collector regions are replaced with SiO_2 . This forces the collector current to flow solely in the vertical direction below the intrinsic base, hence the name collector transistor.

A PISCES simulation predicted the multidimensional current flow (Fig. 3.16). This diagram displays the PISCES simulation of the electron current density-vector plot of the advanced BJT biased at $V_{CE} = 2.0$ V and $V_{BE} = 0.9$ V ($I_c :::: 0.5$ mNj,.lm). In the high-current mode, excess carriers are injected into the epitaxial collector (base pushout). The excess electrons diffuse laterally in the epilayer collector under the extrinsic base due to high carrier concentration gradients in the horizontal direction. Collector current

REFERENCES

- [1] Konaka, S., Y. Yamamoto, and T. Sakai (1986), IEEE Trans. Electron Devices ED-33, 626.
- [2] Tang, D. D., T.-C. Chen, C.-T. Chuang, G. P. Li, M. C. Stork, M. B. Ketchen, E. Hackbarth, and T. H. Ning (1987), IEEE Electron Device Lett. EDL-8, 174., S. 1997
- [3] Li, G. P., E. Hackbarth, and T.-C. Chen (1988), IEEE Trans. Electron Devices ED-35, 89.
- [4] Zaroni, E., E. F. Crabbe, I. M. C. Stork, P. Pavan, G. Verzellesi, L. Vendrame, and C. Canali (1993), IEEE Electron Device Lett. EDL-14, 69.
- [5] Roulston, D. J. (1990), Bipolar Semiconductor Devices (McGraw Hill, New York).
- [6] Sze, S. M. (1988), VLSI Technology, 2nd ed. (McGraw Hill, New York).
- [7] J. S. Yuan, (1999) SiGe, GaAs, and InP Heterojunction Bipolar Transistors, Wiley, New York
- [8] B. G. Streetman and S. Banerjee, (2000) Solid State Electronic Devices, 5th ed. Upper Saddle River: Prentice Hall.

